Eur. Phys. J. B (2015) 88: 254
DOI: 10.1140/epjb/e2015-60314-0

THE EUROPEAN PHYSICAL JOURNAL B

Regular Article

Clustering and phase synchronization in populations of coupled phase oscillators

Guadalupe Cascallares[1,2,a] and Pablo M. Gleiser[1,2]

[1] Centro Atómico Bariloche, Bariloche, 8400 Río Negro, Argentina
[2] Consejo Nacional de Investigaciones Científicas y Técnicas, Buenos Aires, Argentina

Received 21 April 2015 / Received in final form 21 August 2015
Published online 12 October 2015 –

Abstract. In many species daily rhythms are endogenously generated by groups of coupled neurons that play the role of a circadian pacemaker. The adaptation of the circadian clock to environmental and seasonal changes has been proposed to be regulated by a dual oscillator system. In order to gain insight into this model, we analyzed the synchronization properties of two fully coupled groups of Kuramoto oscillators. Each group has an internal coupling parameter and the interaction between the two groups can be controlled by two parameters allowing for symmetric or non-symmetric coupling. We show that even for such a simple model counterintuitive behaviours take place, such as a global decrease in synchrony when the coupling between the groups is increased. Through a detailed analysis of the local synchronization processes we explain this behaviour.

1 Introduction

As an adaptation to cyclic environmental changes many species present behavioural and physiological rhythms with a period close to 24 h, known as circadian rhythms. This daily rhythms are endogenously generated, and continue to oscillate even in the absence of any environmental cues. The generation of circadian oscillations takes place at the individual cell level, and is driven by transcriptional-translational negative feedback loops. Behavioural rhythms are controlled by groups of intercommunicating neurons, which act as pacemakers. These neurons receive information from the environment (such as light, temperature, etc.) and transmit it for entrainment to downstream oscillators [1].

Many animals present two bouts of activity, with peaks that anticipate the morning and the evening. In 1976 Daan and Pittendrigh [2] proposed that these peaks have a neuronal basis, and are driven by two separate oscillators with different responses to light. The morning (M) oscillator is accelerated by light and synchronized by dawn, while the evening (E) oscillator is slowed down by light and synchronized to dusk. This model allows for seasonal adaptation, increasing or decreasing the distance between the peaks of activity according to day length. There is evidence for and against this model, both in mice and flies, which are two of the most important models in chronobiology [3].

In *Drosophila*, the fruit fly, the circadian clock is composed by 150 neurons organized in very few clusters. The clock pacemakers neurons can be divided into two main groups, lateral neurons (LN), also subdivided into dorsal lateral neurons (LN_d) and ventral lateral neurons (LN_v), and dorsal neurons (DN) [4]. Stoleru et al. [5] proposed that LN_v neurons function as the M oscillator, while the E peak is controlled by LN_d neurons. Much detail in known on the circadian oscillations of individual cells in this neural network. However, understanding the underlying molecular details of the coupling between few cells still remains a challenging task [6,7].

In mammals the pacemaker neurons are located in the suprachiasmatic nucleus (SCN) of the brain. The SCN is formed by two lobes, which can be divided in a ventrolateral core and a dorso-medial shell region. The core receives information from the environment, mainly from the retino-hypothalamic tract and transmits this information to the shell. The synchronization properties of these groups of neurons are different. The oscillations in clock gene expression in the core present a low amplitude, which allows for entrainment with the environmental cues. On the other hand, gene expression in the shell presents robust circadian oscillations, allowing for sustained oscillations in the absence of environmental cues. Also, the core and the shell express different neurotransmitters to synchronize their signals. Core neurons use vasoactive intestinal peptide (VIP) to transmit the information, while the shell contains populations of neurons using arginine vasopressin (AVP) for communication. Experimental evidence supports the idea that both anatomical organization and cell to cell communication allows for coupling and synchronization between the neurons, in order to generate coordinated rhythms in the SCN [8].

[a] e-mail: gcascallares@cab.cnea.gov.ar

Motivated by these experimental results we want to see if changes on neuronal synchronization could be a consequence of structural changes in the network, such as coupling, number of oscillators and time delay. We consider a system formed by two groups of fully coupled phase oscillators whose natural frequencies are bimodally distributed. By changing the coupling between the oscillators we show the emergence of different synchronized clusters. We will focus our work on computational simulations, taking into account finite size effects and also frequency distributions that are not symmetric. Even for such a simple system we show that counterintuitive behaviours can take place, in particular we show that in some cases increasing the coupling between the oscillators can hinder global synchronization.

2 The model

We model rhythmic circadian units with phase oscillators, whose periodic dynamic is described by a single variable, its phase ϕ. These models have been extensively studied, with diverse applications involving physical, technological and biological systems (see [9–14] and references therein).

Perhaps the most studied model is the one proposed by Kuramoto [9], where the interaction between the oscillators is a periodic function of the phases:

$$\frac{d\phi_i}{dt} = \omega_i + \frac{k}{N}\sum_{j=1}^{N}\sin\left(\phi_j - \phi_i\right), \tag{1}$$

where $i = 1, \ldots, N$, ω_i is the natural frequency of oscillator i and k is the coupling strength. This model presents a phase transition at a critical value of the coupling, k_c, where a single cluster of synchronized oscillators emerges.

In this work we use a model of two coupled groups of phase oscillators. The route to synchronization of two coupled ensembles of oscillators was first studied in reference [15] where Okuda and Kuramoto considered coupled populations of identical phase oscillators under noise. This model was also investigated to find different routes to synchronization, including asymmetry in the coupling strength between the groups [16,17], considering different frequency distributions [18], to describe chimera states [19] and as an application to epileptic seizures [20]. Here we will focus our interest in this model analyzing the role of the interactions in the synchronization properties of the model. In particular, we will consider the effects of asymmetric distributions, finite-sized systems and time delays. As stressed by Martens et al. [21] these ingredients strongly limit analytical analysis and thus we will focus on numerical simulations.

The system is formed by two types of oscillators with phases $\phi_i^{(1)}$ and $\phi_j^{(2)}$ which are fully coupled with intragroup coupling k_i $(i = 1, 2)$ and intergroup coupling k in one direction and qk in the other one. τ is the time delay between groups. When $k = 0$, the two groups are uncoupled, so the synchronization property of each group is independent of the other, and depends only on their intragroup couplings k_1 and k_2. The asymmetric coupling allows for a change of roles between groups, and by fixing the parameter q we can analyze how one group influences the other. Coupling is modeled as a mean field, and the interaction is global (all-to-all). The equations for the dynamics are:

$$\frac{d\phi_i^{(1)}}{dt} = \omega_i{}^{(1)} + \frac{k_1}{N_1}\sum_{j=1}^{N_1}\sin\left(\phi_j{}^{(1)}(t) - \phi_i{}^{(1)}(t)\right) + \frac{qk}{N_2}\sum_{j=1}^{N_2}\sin\left(\phi_j{}^{(2)}(t-\tau) - \phi_i{}^{(1)}(t)\right) \tag{2}$$

$$\frac{d\phi_i^{(2)}}{dt} = \omega_i{}^{(2)} + \frac{k_2}{N_2}\sum_{j=1}^{N_2}\sin\left(\phi_j{}^{(2)}(t) - \phi_i{}^{(2)}(t)\right) + \frac{k}{N_1}\sum_{j=1}^{N_1}\sin\left(\phi_j{}^{(1)}(t-\tau) - \phi_i{}^{(2)}(t)\right). \tag{3}$$

We use a normalized Gaussian distribution of natural frequencies

$$g(\omega) = \frac{1}{\sqrt{2\pi\sigma^2}}\exp\frac{-(\omega-\omega_0)^2}{2\sigma^2}, \tag{4}$$

where each group has a different mean value of the frequencies distribution $\omega_0^{(1)}$ and $\omega_0^{(2)}$. The model allows for analytic analysis, and the critical coupling for each group can be shown to be $k_c = 2/[\pi g(\omega_0)]$ [9,11–14].

Interacting populations of Kuramoto-type oscillators have been intensively studied in several recent works. In particular, the Ott-Antonsen ansatz [22] for Kuramoto-type oscillators with Lorentzian frequency distribution greatly facilitated theoretical analysis of such models. Using this ansatz, in reference [21], the bifurcation analysis for the system on the infinite-N limit was done.

In order to quantify the synchronization of each subsystem we use the Kuramoto order parameter

$$r_{(1,2)}e^{i\Phi_{(1,2)}} = \frac{1}{N}\sum_{j=1}^{N}e^{i\phi_j^{(1,2)}}, \tag{5}$$

where $r(t)$ gives a measure of the coherence of the oscillators $(0 \le r \le 1)$, and $\Phi(t)$ is the average phase.

We characterize the global phase synchronization using the global order parameter S [20]

$$S = \frac{1}{T}\int_{T_0}^{T_0+T}\left|\frac{r_1 e^{i\Phi_1} + r_2 e^{i(\Phi_2+\Phi^*)}}{2}\right| dt, \tag{6}$$

where Φ^* is the most probable phase difference for a period T, which can be measured from the maximum of the probability density distribution of the cyclic phase difference $\Delta\Phi(t) = \mathrm{mod}(\Phi_1(t) - \Phi_2(t), 2\pi)$ [23]. When both groups are phase-locked, S is the mean of r_1 and r_2, but if there is no phase locking S is expected to be small.

In order to analyze the formation of locally synchronized clusters we also measure the frequency synchronization of each group, which is quantified using the mean

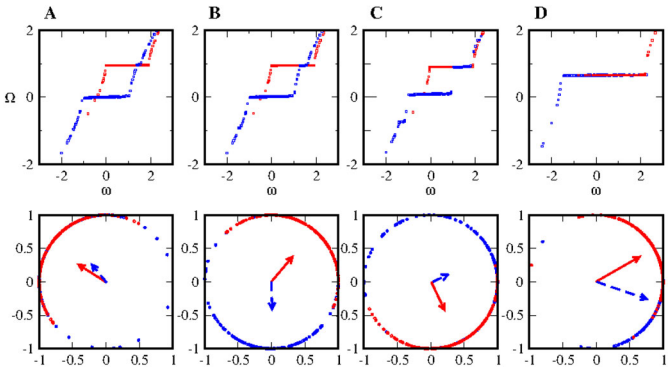

Fig. 1. (Top row) Mean frequency Ω_i as a function of natural frequency ω_i for oscillators in group 1 (blue) and 2 (red) for four different intergroup coupling strengths: (A) $k = 0.05$, (B) $k = 0.1$, (C) $k = 0.2$, (D) $k = 0.5$. Synchronized oscillators appear as horizontal lines. (Bottom row) Snapshots of phases for the synchronized clusters. The vectors show the value of the phase synchronization order parameter for each group. All figures correspond to parameters $k_1 = 1.8$, $k_2 = 1.4$, $q = 2$, $\sigma_1 = 1$, $\sigma_2 = 0.5$, and $\Delta\omega = \omega_0^{(2)} - \omega_0^{(1)} = 1$.

oscillation frequency Ω, calculated over a time interval of length T,

$$\Omega_{(1,2)} = \frac{1}{T}\int_t^{t+T} \dot{\phi}_i^{(1,2)}(t')dt'. \quad (7)$$

3 Results

In the top row of Figure 1 we plot the mean frequency Ω as a function of the natural frequency ω for oscillators in group 1 (blue) and 2 (red) for four different intergroup coupling strengths. The figures clearly show the presence of synchronized clusters, which appear as horizontal lines. These are oscillators with different natural frequencies that now have the same mean frequency. Both groups have an intracoupling greater than the critical value, thus, as expected, a synchronized cluster emerges with mean frequency $\Omega_{(1,2)}$, centered in the mean value of the frequency distribution ($\omega_0^{(1,2)}$). Even for low intercoupling some oscillators of group 1 synchronize their frequencies with the mean frequency $\omega_0^{(2)}$. This can be observed as a small blue cluster in the middle of the horizontal red line in the first panel, when $k = 0.05$. The first oscillators to synchronize are those with natural frequencies close to Ω_2. As the intergroup coupling is increased further more oscillators join this cluster. This effect can be reversed by tuning the parameter q. For example, for $q = 0.5$ the results are qualitatively the same, however, in this case the oscillators of group 2 jump to the cluster centered in Ω_1.

An interesting effect can be observed for $k = 0.2$ in Figure 1C, where a "resonance" effect takes place. A small cluster of oscillators is observed to emerge close to $\Omega = -0.5$. The formation of clusters with different average frequencies is usually observed in systems locally connected or with a given network structure [13,23]. However, they also appear in fully connected systems when the heterogeneities are not in the network structure, but in the coupling strength [24–26]. These clusters were observed experimentally in groups of chemical interacting oscillators that could be described as Kuramoto phase oscillators with multi-peaked frequency distributions by Kiss and coworkers [20,27]. It is important to highlight the formation of these structures despite the fact that this is a mean-field model. From a biological point of view, these structures could be required to encode or allow for the emergence of different hierarchies by changing the coupling. In fact, it has been observed that coupling between the neurons plays an important role in the SCN to ensure a robust but flexible circadian system [28]. As the intergroup coupling is increased further the oscillators in both groups synchronize at the same mean frequency, and finally a single synchronized cluster formed both by oscillators of group 1 and 2 is observed.

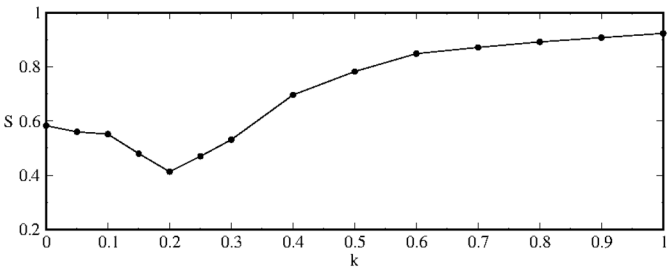

Fig. 2. The global phase synchronization order parameter S as a function of intergroup coupling k. S presents a non-monotonous behaviour as a function of k. The figure corresponds to parameters $k_1 = 1.8$, $k_2 = 1.4$, $q = 2$, $\sigma_1 = 1$, $\sigma_2 = 0.5$, and $\Delta\omega = 1$.

On the bottom row of Figure 1 we present snapshots of the phases of the oscillators distributed on the unit circle. For clarity we only show those oscillators in the largest synchronized cluster. We also plot the Kuramoto order parameter for each group as vectors. The length of the arrows represents the degree of phase synchronization, and the direction points towards the mean phase. In order to compare the four snapshots we use the same initial conditions. For $k = 0.05$ the phase synchronization in group 2 is clearly larger than in group 1. As the intercoupling is increased the order parameter in group 1 seems to slowly increase ($k = 0.1$) and then seems to decrease ($k = 0.2$). Eventually both groups become synchronized at the same mean frequency and both order parameters increase showing, as expected, that a phase synchronization takes place. This phenomenon is due to the asymmetry between the clusters introduced by q. Note how the non-synchronized oscillators of both groups 1 and 2, which are close to the main cluster of group 2, synchronize with the main cluster in Ω_2. At the coupling is increased further more oscillators synchronize with this cluster. Also, the final average frequency Ω does not match exactly Ω_2 since there are still non-synchronized oscillators which modify this efective frequency.

In order to quantitatively characterize the global phase synchronization we show in Figure 2 the behaviour of S

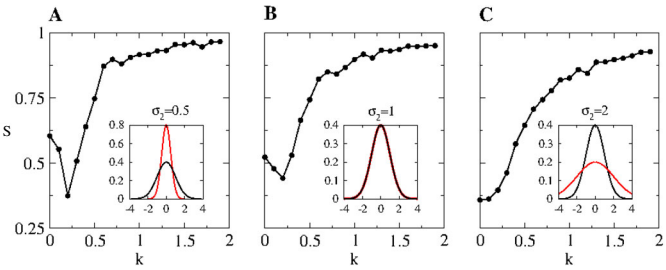

Fig. 3. Global phase synchronization order parameter S vs. intergroup coupling k for three different standard deviations of the Gaussian frequency distribution of group 2: (A) $\sigma_2 = 0.5$, (B) $\sigma_2 = 1.0$, (C) $\sigma_2 = 2.0$. In group 1 we fixed $\sigma_1 = 1.0$. The figures correspond to $k_1 = 1.8$, $k_2 = 1.8$, $q = 2$, and $\Delta\omega = 1$. As the intracoupling becomes greater than the critical coupling the minimum in the order parameter becomes sharper.

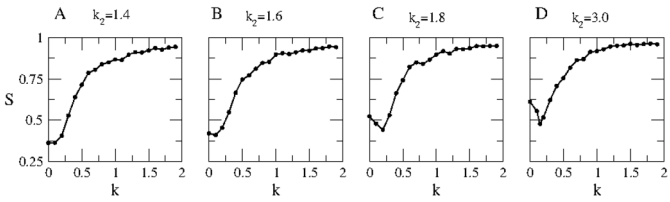

Fig. 4. The global phase synchronization parameter S vs. intergroup couplings k for four different intragroup couplings of group 2, (A) $k_2 = 1.4$, (B) $k_2 = 1.6$, (C) $k_2 = 1.8$ and (D) $k_2 = 3.0$. All figures correspond to parameters $\sigma_1 = 1$, $k_1 = 1.8$, $q = 2$, $\Delta\omega = 1$ and 100 independent simulations.

as a function of intergroup coupling k. We find that S presents a non-monotonous behaviour. For $k = 0$ the order parameter has a high value $S \approx 0.6$, which is expected since both groups have intragroup coupling above the critical value k_c and synchronized clusters are already present in the system. For small intergroup coupling ($k < 0.1$) the effect on global synchronization is small, even when a decrease in S can already be observed. As k is increased further S decreases, eventually reaching a minimum for $k \approx 0.2$, and then increases monotonously with k.

A non-monotonous behaviour of the phase order parameter (Eq. (5)) has been observed in the Kuramoto model when the natural frequencies are randomly allocated in diluted network structures, such as random and scale-free networks [29]. This effect is due to the local synchronization for low coupling among neighbouring oscillators with similar natural frequencies. As the coupling is increased this locally synchronized groups interact and become synchronized among themselves, leading to higher values of the order parameter.

In our model the system is fully coupled and the non-monotonous behaviour arises from the competition between synchronized clusters of oscillators 1 and 2. As it was observed before, when $k \approx 0.2$ the oscillators of group 1 are jumping to the synchronized cluster of group 2, leading to a decrease in the value of the parameter order of group 1. This affects the global synchronization, until the size of the main cluster becomes sufficiently large.

We will focus our attention now on the role of the widths of the natural frequency distributions of each group, which are expected to have a direct relation with the size of the synchronized clusters, since they change the value of the critical coupling. Up to now we have presented results where the standard deviation of the Gaussian frequency distribution for group 1 was $\sigma_1 = 1.0$, while for group 2 it was $\sigma_2 = 0.5$, so the critical values were $k_c^{(1)} \approx 1.59$ and $k_c^{(2)} \approx 0.79$. We will analyze now the effect of changing σ_2 while maintaining the standard deviation of group 1 fixed to $\sigma_1 = 1.0$. In Figure 3 we plot S vs. k for: (A) $\sigma_2 = 0.5$ and $k_2 \gg k_c^{(2)}$, (B) $\sigma_2 = 1.0$ and $k_2 > k_c^{(2)}$ and (C) $\sigma_2 = 2.0$ and $k_2 < k_c^{(2)}$. As a guide to the eye we also show the qualitative shape of the distributions (in black the group with σ_1 and in red the group with σ_2). The parameters were fixed to $k_1 = 1.8$, $k_2 = 1.8$, $q = 2$ and $\Delta\omega = 1$.

When the intracoupling of group 2 is much greater than $k_c^{(2)}$, as in Figure 3A, the non-monotonous behaviour is sharper. Note that also $S^A_{\min} > S^B_{\min}$. As σ_2 is increased the non-monotonous behaviour is smoothed further, and as Figure 3C shows, for $\sigma_2 = 2.0$ the order parameter S presents a monotonous behaviour. Note that in this case, for $k = 0$, the value of S is much smaller than the one observed in Figure 3A. This is due to the largest standard deviation value of σ_2 that hinders the formation of synchronized clusters for the same intracoupling $k_2 = 1.8$.

Next, we analyze the role of the intragroup coupling taking into account the heterogeneity in the distribution of natural frequencies of the different groups. In Figure 4 we show the global order parameter S as a function of the intergroup coupling k for four different values of k_2 when $\sigma_1 = \sigma_2 = 1.0$. If $k_2 \leq k_c$ (first column), S has a monotonous behaviour. Otherwise, synchronization in group 1 is strong enough as not to be influenced by group 2, and there is no competition between synchronized clusters. If $k_2 > k_c^{(2)}$, a clear non-monotonous behaviour is observed. Note that for $k = 0$, the value of S is increased as the value of k_2 is increased. This phenomenon is a consequence of the wider distribution of frequencies that hinders synchronization.

We also analyze the effect of changing the size of one group while the size of the other group is fixed. In Figure 5 we show results when the size of group 2 is fixed to $N_2 = 200$ and the size of group 1 is varied to (A) $N_1 = 40$, (B) $N_1 = 80$ and (C) $N_1 = 160$. We plot the average frequency as a function of the natural frequency ω for individual oscillators. Note that the same qualitative behaviour is observed in the three cases. For very small k two different synchronized clusters can be clearly distinguished. As k is increased oscillators in group 1 move to the largest cluster initially formed by oscillators in group 2. For sufficiently large k all oscillators are synchronized in a single cluster.

In Figure 6 we show the temporal evolution of the phase for 15 oscillators in each of the synchronized clusters observed in Figure 5. The figure shows how the phase relationship between the groups can be tuned by keeping the coupling strength between the groups fixed and changing the number of oscillators in each group. Remarkably,

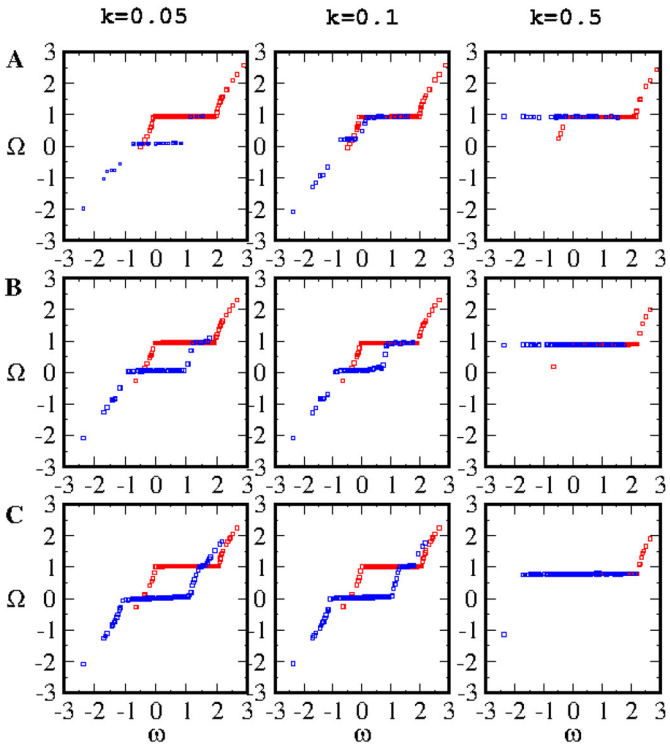

Fig. 5. Average frequency Ω as a function of natural frequency ω for three different sizes of group 1 and three different coupling strengths: (A) $N_1 = 40$, (B) $N_1 = 80$ and (C) $N_1 = 160$. The size of group 2 was fixed to $N_2 = 200$. The figures correspond to $k_1 = 1.8$, $k_2 = 1.4$, $q = 2$ and $\Delta\omega = 1$. Note that similar frequency synchronized clusters are observed in the three cases.

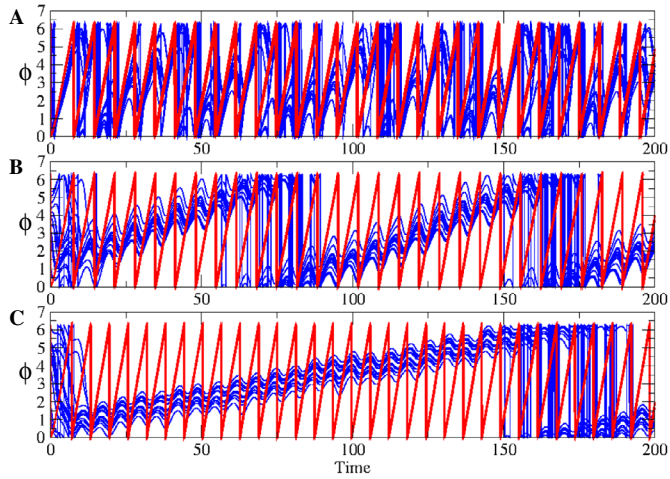

Fig. 6. Temporal evolution of the phase for 15 oscillators in each of the synchronized clusters observed in Figure 5, for (A) $N_1 = 40$ (B) $N_1 = 80$ (C) $N_1 = 160$ when $k = 0.1$.

experimental observations suggest that subpopulations among SCN cells show multiple phase relationships that could contribute to photoperiodic adaptation [30].

It has been also observed that the two hemispheres in the SCN can split their activity and oscillate oppositely in antiphase [31]. Li et al. [32] showed that time delay is a

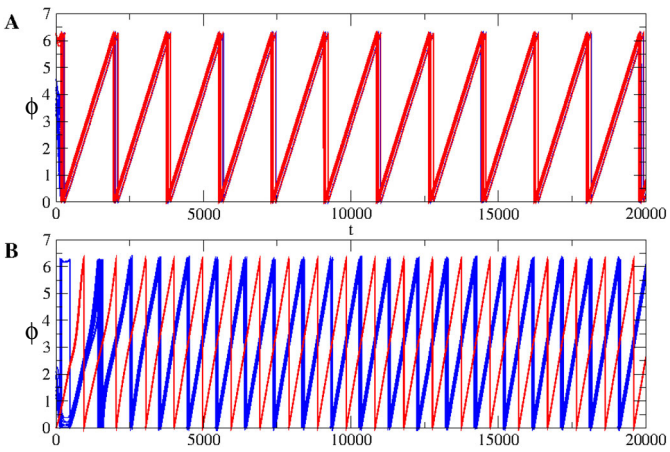

Fig. 7. Evolution of the phase of 10 oscillators in the largest synchronized cluster. All systems start with identical initial conditions but different time delays: (A) $\tau = 0$ and (B) $\tau = 4$. When there is no time delay, both groups are synchronized in phase and frequency, but when $\tau = 4$, there is an antiphase behaviour. The value of the parameters are $k_1 = 1.8$, $k_2 = 1.4$, $q = 2$, $\sigma_1 = 1.0$, $\sigma_2 = 0.5$, $\Delta\omega = 1$.

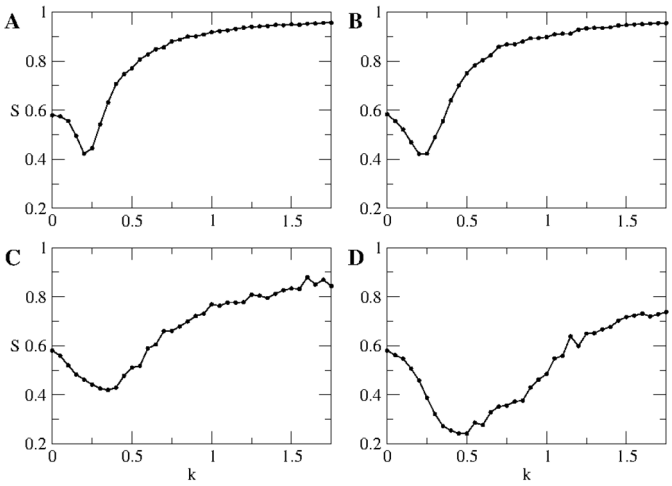

Fig. 8. Order parameter S as a function of the intergroup coupling k for: (A) $\tau = 0$, (B) $\tau = 2$, (C) $\tau = 4$ and (D) $\tau = 6$. For larger values of time delay, the non monotonous behaviour is less sharp. Parameters have the same values as Figure 7.

key factor in order to get antiphase oscillation patterns. So now we are going to consider $\tau \neq 0$. In Figure 7 we show that we can achieve this antiphase pattern by tuning the time delay between the groups. When there is no delay, both groups oscillate in phase, but if we increase τ we can get antiphase behaviour with the same initial conditions and parameters.

Next, we analyzed the effect of delay in the global synchronization of the system. In Figure 8 we plot the order parameter S as a function of intergroup coupling k for four different values of time delay τ and 500 independent realizations. As in the case with $\tau = 0$ a non monotonous behaviour can be clearly observed. However, the presence

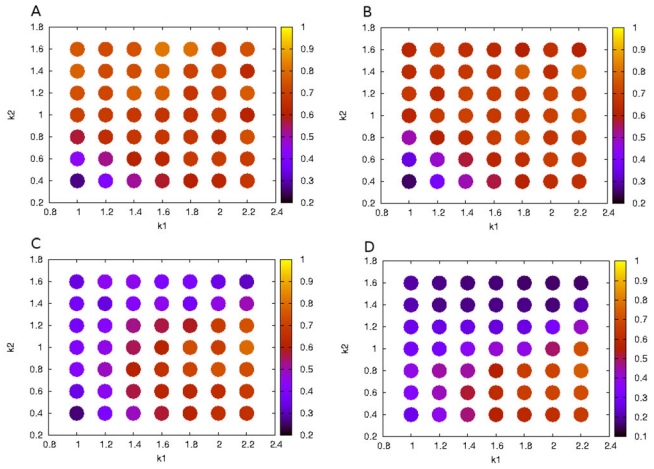

Fig. 9. The color indicates the value of the order parameter S for: (A) $\tau = 0$, (B) $\tau = 2$, (C) $\tau = 4$ and (D) $\tau = 6$. In these k_1-k_2 diagrams it is possible to see how the region of stronger synchronization changes according to the time delay. For larger delays, the synchronization region is smaller and a stronger coupling in group 2 does not ensure global synchronization. The figures correspond to $k = 0.5$, $q = 2$, $\sigma_1 = 1.0$, $\sigma_2 = 0.5$, $\Delta\omega = 1$ and 10 simulations.

of a delay is detrimental for global synchronization. As τ increases, the trough decreases and also for larger couplings S presents smaller values. Also, for larger delays, the system presents stronger fluctuations which are reflected in the behaviour of the order parameter.

Figure 9 illustrates the regions of global synchronization for four different time delays with $k = 0.5$. We find that the synchronization region reduces with increasing values of τ. In (A), almost for any intragroup coupling the system has a high global order parameter value, including values both above and below the critical intragroup coupling. Note also that, as the time delay increases, for example in (D), the synchronization region is limited almost to intragroup coupling for group 2 below its critical value ($k_c^{(2)} \approx 0.79$).

4 Summary

Our work was motivated by behaviours observed in the circadian pacemaker neurons of the fly and mammals. Specific groups of neurons, labeled as morning (M) and evening (E) oscillators, track dawn and dusk and thus allow for anticipation of activity in the morning and evening. An interesting open question is related to the fact that behavioural outputs such as locomotor activity are not necessarily correlated with the synchronization properties of a single neuronal group, and rather seem to depend on the interactions between these neuronal groups [6,7]. In the brain of the fly, the neuropeptide pigment-dispersing factor (PDF) plays the role of a synchronizing factor [33], coupling the circadian oscillations of the clock neurons. A similar role is played in mammals by vasoactive intestinal polypeptide (VIP). The role that PDF and VIP play is far from trivial, for example, PDF can shorten or lengthen the period of specific clock neurons in a dose-dependent manner [34]. In order to gain insight into this problem we analyzed the synchronization properties of two fully coupled groups of Kuramoto oscillators. Using numerical simulations we studied how different coupling intensities between the two groups affects global and local synchronization. We showed that even for such a simple model counterintuitive results can emerge, and in some conditions increasing the coupling between the oscillators can hinder global synchronization. We showed that this is due to the emergence of frequency synchronized clusters, whose competition leads to a non-monotonous behaviour of the global order parameter. We analyzed the dispersion of natural frequencies and different intergroup couplings and showed under which condition the global order parameter presents a monotonous or non-monotonous behaviour. Finally we showed how the phase relation between frequency synchronized clusters can be tuned by changing the number of oscillators in each group and the time delay.

The authors gratefully acknowledge financial support from CONICET (Project PIP 11220120100495).

References

1. *Clocks and Rhythms*, in *Cold Spring Harbor Symposia on Quantitative Biology* (Cold Spring Harbor Laboratory Press, 2008), Vol. 72
2. S. Daan, C.S. Pittendrigh, J. Comp. Physiol. **106**, 253 (1976)
3. C. Helfrich-Förster, J. Biol. Rhythms **24**, 259 (2009)
4. V. Sheeba, M. Kaneko, V. Sharma, T. Holmes, Crit. Rev. Biochem. Mol. Biol. **43**, 37 (2008)
5. D. Stoleru, Y. Peng, J. Agosto, M. Rosbash, Nature **431**, 862 (2004)
6. Z. Yao, O.T. Shafer, Science **343**, 1516 (2014)
7. S. Risau Gusman, P. Gleiser, J. Biol. Rhythms **29**, 401 (2014)
8. M. Hafner, H. Koeppl, D. Gonze, PLoS Comput. Biol. **8**, e1002419 (2012)
9. Y. Kuramoto, *Chemical Oscillations, Waves and Turbulence* (Springer, 1984)
10. T. Winfree, *The Geometry of Biological Time*, Interdisciplinary Applied Mathematics (Springer, 2001)
11. A. Pikovsky, M. Rosenblum, J. Kurths, *Synchronization. A Universal Concept in Nonlinear Sciences* (Cambridge University Press, 2001)
12. S. Strogatz, *Sync. The Emerging Science of Spontaneous Order* (Hyperion, 2003)
13. S. Manrubia, A. Mikhailov, D. Zanette, *Emergence of Dynamical Order. Synchronization Phenomena in Complex Systems* (World Scientific, 2004)
14. J. Acebrón, L. Bonilla, C.P. Vicente, F. Ritort, R. Spigler, Rev. Mod. Phys. **77**, 137 (2005)
15. K. Okuda, Y. Kuramoto, Prog. Theor. Phys. **86**, 1159 (1991)
16. E. Montbrió, J. Kurths, B. Blasius, Phys. Rev. E **70**, 056125 (2004)

17. J. Sheeba, V. Chandrasekar, A. Stefanovska, P. McClintock, Phys. Rev. E **78**, 025201 (2008)
18. E. Barreto, B. Hunt, E. Ott, P. So, Phys. Rev. E **77**, 036107 (2008)
19. D. Abrams, R. Mirollo, S. Strogatz, D. Wiley, Phys. Rev. Lett. **101**, 084103 (2008)
20. I. Kiss, M. Quigg, S.H. Chun, H. Kori, J. Hudson, Biophys. J. **94**, 1121 (2008)
21. E.A. Martens, E. Barreto, S.H. Strogatz, E. Ott, P. So, T. Antonsen, Phys. Rev. E **79**, 026204 (2009)
22. E. Ott, T. Antonsen, Chaos **18**, 037113 (2008)
23. I. Kiss, Y. Zhai, J. Hudson, Science **296**, 1676 (2002)
24. H. Sakaguchi, Prog. Theor. Phys. **79**, 39 (1988)
25. J.R. Engelbrecht, R. Mirollo, Phys. Rev. Lett. **109**, 034103 (2012)
26. D. Pazo, E. Montbrio, Phys. Rev. X **4**, 011009 (2014)
27. A. Mikhailov, D. Zanette, Y. Zhai, I. Kiss, J. Hudson, Proc. Natl. Acad. Sci. **101**, 10890 (2004)
28. U. Abraham, A. Granada, P. Westermark, M. Heine, A. Kramer, H. Herzel, Mol. Syst. Biol. **6**, 438 (2010)
29. L. Buzna, S. Lozano, A. Díaz-Guilera, Phys. Rev. E **80**, 066120 (2009)
30. J. Schaap, H. Albus, H.T. vanderLeest, P. Eilers, L. Détári, J. Meijer, Proc. Natl. Acad. Sci. **100**, 15994 (2003)
31. H. de la Iglesia, J. Meyer, A. Carpino Jr, W. Schwartz, Science **290**, 799 (2000)
32. D. Li, C. Zhou, Frontiers Syst. Neurosc. **5**, 100 (2011)
33. T. Yoshii, C. Wülbeck, H. Sehadova, S. Veleri, D. Bichler, R. Stanewsky, C. Helfrich-Förster, J. Neurosci. **29**, 2597 (2009)
34. C. Wülbeck, E. Grieshaber, C. Helfrich-Förster, J. Biol. Rhythms **23**, 409 (2008)